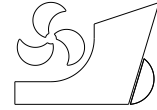


Ahmet Ziya Saydam
Gözde Nur Küçüksu
Mustafa İnsel
Serhan Gökçay



<http://dx.doi.org/10.21278/brod73406>

ISSN 0007-215X
eISSN 1845-5859

UNCERTAINTY QUANTIFICATION OF SELF-PROPULSION ANALYSES WITH RANS-CFD AND COMPARISON WITH FULL-SCALE SHIP TRIALS

UDC 629.5.035:629.5.016.7:629.5.018.75

Original scientific paper

Summary

RANS-CFD is a well-established tool with widespread use in maritime industry and research. Valuable information might be extracted from the results of such simulations in terms of ship resistance and flow field variables. With recent advancements in computational power, it became possible to investigate the performance of ships in self-propulsion conditions with RANS method. This paper presents the results of a study in which self-propulsion analyses of a small size product/oil tanker has been carried out at ship scale. The methodology proposed in this study makes use of open water propeller performance predictions, resistance analyses at model scale and self-propulsion computations at ship scale for a minimum of 2 different propeller loadings to obtain the self-propulsion point and respective performance parameters. In order to speed up the time-consuming self-propulsion computations, these cases have been solved with a single-phase approach. Resistance predictions have been compared with experimental findings. Uncertainty associated with prediction of resistance and thrust has been quantified. Additionally, sea trials have been conducted on the subject vessel and its two sisters and measured delivered power data have been used for evaluating the capability of the numerical method in self-propulsion predictions. Comparison of results indicate that the proposed self-propulsion computation methodology with RANS CFD at ship scale is capable of predicting delivered power with sufficient accuracy at an acceptable computational cost.

Key words: CFD; RANS; full-scale; uncertainty; self-propulsion

1. Introduction

Viscous computational fluid dynamics analyses utilizing RANS method has become a reliable tool that has been incorporated to the design process of ships. Whilst the method enables the comparison of numerous design alternatives with measurably lower cost compared to experimentation, it also is useful in providing valuable information regarding the flow around the ship that is of vital importance for design improvement such as streamlines, velocity vectors, pressure level information and etc. The wave formation around the hull, spray formation (if

any), dynamic attitude (sinkage and trim) and wake distribution are among the vital information that may be reproduced from RANS CFD studies with high-fidelity. Resistance characteristics of ships may also be evaluated with high accuracy as the uncertainty of RANS method has been quantified and results are validated against experimental data [1].

Currently, the extent of RANS CFD analyses for ship design is being expanded to account for the propulsion performance of the vessels. The contributions to the literature about self-propulsion performance estimations of ships with CFD have been increasing in the last decade in proportion with the advance of modelling techniques and improvement in computational power.

Ponkratov and Zegos [2] have analysed the propulsion performance of a fully appended medium range tanker. Model scale CFD results were compared with the towing tank test results, and the ship scale CFD data was compared with sea trials and ITTC-78 based estimations. The results of torque, thrust and power were compared with both sea trials and ITTC-78 method based on the model test. Results indicate that full scale CFD method results in less error compared to model scale computations.

Kınacı, Gokce, Alkan and Kukner [3] have conducted a case study in which self-propulsion computations of three different ships have been done by RANS CFD. Results obtained with the sliding mesh approach were found to be in accordance with results from literature. Virtual disk method has also been applied: although satisfactory results have been obtained for the DARPA Suboff, the results for KCS and DTC were not in good agreement with the literature.

Mikkelsen, Steffensen, Ciortan, and Walther [4] have analysed towing tank test data, model scale and ship scale CFD, sea trials and in-service performance data of a bulk carrier. The validation of the model scale CFD has been based on towing tank test by means of resistance and self-propulsion simulations. In-service performance data was collected from four sister ships in the first 3-9 months of operation. The extrapolated towing tank test results, sea trials and ship scale CFD data have been compared by means of delivered power. CFD results indicated less overprediction when compared to experiments.

Vukcevic, Jasak, Gatin and Uroic [5] have conducted a comparison of two-phase RANS based CFD analysis at ship scale and sea trial results for a general cargo vessel. CFD simulations make use of pressure-jump actuator-based actuator disc modelling. The comparison with sea trials have been performed in terms of achieved forward speed and dynamic trim for given rpm.

Jasak, Vukcevic, Gatin and Lalovic [6] have made analyses of self-propulsion performance of general cargo and car carrier vessels. Analyses have been performed at ship scale with RANS based CFD and actuator disc modelling. Rpm has been fixed and trim and achieved speed are compared with data obtained from sea trials. Approximately 1.3% under-prediction has been obtained for the forward speed.

Sun, Hu, Hu, Su, Xu, Wei and Huang [7] have studied the propulsion performance of a bulk carrier by RANS based CFD simulations. Statistical sea trial data have been collected from nine new-built ships with same particulars and appendages. The extrapolated towing tank test results have shown 2.4% difference in delivered power compared to sea trials. CFD simulations have predicted delivered power with a difference between -1.1% and 2.4% compared to sea trials.

Mikkelsen and Walther [8] have conducted a study on the comparison of sea trials and ship and model-scale RANS based CFD of a twin-screw ro-ro and a general cargo vessel. The speed trials data have been collected from six sister ships comprised of speed, propeller rate of rotation, and the delivered power data. The CFD simulations for general cargo vessel show 10-14% under-estimation in delivered power compared to speed trials.

Li, Han, Dong, and Zhao [9] have studied the light running margin (LRM) problem of the propeller. The study includes the open water performance analysis and then the trial speed and propeller revolution predictions. The results have been compared to sea trials. The theoretical results have shown about 0.03 knots lower vessel speed and 1.8 *rpm* higher propeller rotational speed compared to sea trials.

Hasselaar and Kaeding [10] have compared full scale RANS-BEM coupling method based CFD simulations and model tests to validate the performance energy saving devices (ESD). The full-scale CFD simulations and sea trials have been compared by means of the non-dimensionalised power and speed correlation. The calculation has been performed with/without ESD by considering propeller blade roughness. The prediction of delivered power difference between sea trials and CFD simulation has been reduced to 8% by considering the propeller roughness.

Kamal, Shamsuddin and Binns [11] have compared full scale CFD simulation with sea trials and the towing tank test results by means of delivered power. In the CFD analysis of the training vessel, actuator disk modelling has been used for propeller model. Sea trials results are in good agreement with the towing tank test results, where the CFD simulation has underpredicted the delivered power compared to towing tank results.

Dogrul [12] has conducted a numerical study on the scale effects associated with the propulsion performance of Joubert BB2 submarine equipped with MARIN7371R propeller with RANS method. Body force method was used for self-propulsion computations. Scale effect on the wake fraction was found to be excessive when compared to thrust deduction.

Dai et al [13] have conducted a numerical study to obtain propulsion parameters in regular head and oblique waves with RANS method. Self-propulsion simulations in calm water and waves have been performed. The effect of waves on thrust deduction and wake fraction, open water, relative rotative, hull and propulsive efficiencies are discussed.

There are several verification studies for propulsion performance prediction of various ship types by RANS CFD in the literature. Generally, the studies are based on Richardson extrapolation [7], [8], [14], [15]. Applications utilizing the safety factor method are also present [6].

Farkas et al [16] have conducted experimental and numerical studies on a handymax bulk carrier. Numerical studies were conducted with RANS method in multi-phase configuration. Body force method has been used for including the propeller effect during computations. Verification and validation analyses were conducted by utilizing extrapolated experimental data. Effect of different turbulence modelling methods on results were also investigated. Although their results indicate superiority of Reynolds Stresses Model for turbulence modelling, additional computation time required for solving the extra equations is found as a disadvantage of the approach.

Farkas et al [17] have further investigated the capabilities of RANS based CFD in predicting the wake field of a ship. Results were validated with experimental data at model scale. Wall function approach was found to predict the ship wake satisfactorily. They have observed major scale effects for nominal wake characteristics and recommended that full scale viscous simulations are beneficial in terms of accurate prediction of stern flow characteristics.

Pena and Huang [18] have assessed the suitability of different turbulence models on ship hydrodynamic analyses. Computational effort and accuracy along with applicability have been of primary concern. They concluded that RANS approach with $k-\omega$ SST turbulence modelling is capable of predicting the ship resistance in full scale. They also point out that relatively coarse meshes adopted in RANS approach tend to create inaccuracies associated with flow around propellers.

Terziev et al [19] have reviewed the sources of uncertainties associated with hydrodynamic performance prediction and claimed that although reliable data may be obtained by full-scale ship hydrodynamic simulations, the progress achieved is still not satisfactory to eliminate the need of experimental testing campaigns and extrapolation of data to ship's scale. They identify the main reasons preventing further progress in the field of full-scale computational hydrodynamics as lack of open full-scale data and lack of high computational power.

Having reviewed the literature on propulsive performance prediction of ships with CFD, it can be evaluated that RANS-CFD has become an alternative tool for the purpose along with model experiments. There exist numerous cases in literature where findings from CFD studies are compared with data from model experiments and even full-scale trials. Predictions may tend to underpredict or overpredict the actual delivered power depending on the adopted methodology indicating that a generalized best practice is not existent at this stage. It should also be noted that current and future efforts aiming to reduce the computational effort for finding the self-propulsion point and corresponding performance parameters of a ship with a verified computational approach would make notable contribution to the field of computational hydrodynamics. Full-scale measured data for validating the computational results is seen as a valuable and necessary tool for further progress.

The current research campaign aims to utilize a methodology enabling the prediction of self-propulsion characteristics by a cost-efficient approach while maintaining fidelity. The reduction in computational effort is based on conducting the final self-propulsion analyses in a single-phase configuration rather than simplifying the propeller model. To adopt this cost-effective approach and maintain high-fidelity in the predictions, self-propulsion analyses are conducted at ship's scale and sensitivity of the numerical approach to mesh size and time-step are investigated. Uncertainty associated with calculation of resistance, thrust and torque have been quantified. Results of the analyses have been compared with available full-scale uncertainty data and delivered power measurements conducted during the sea-trials for the subject vessel and its sisters.

2. General information on the pilot ship

In this section, brief information is presented about the tested ship's principal dimensions and powertrain. The tested tanker is shown in Figure 1 and technical details of the ship are presented in Table 1. Two more sister ships have also been tested and delivered power data are available for comparison. The vessel is equipped with a single 2300 kW engine coupled to a gearbox with a reduction ratio of 6.22 and a 4 bladed CPP type propeller. The 3-d hull model is shown in Figure 2 in perspective view.



Fig. 1 Profile view of tested tanker

Table 1 General information on tested tanker

Ship Type	Petrol/chemical tanker
Overall length	109.98 m
Beam	16.60 m
Depth	8.45 m
Draft	6.70 m
Displacement	9060 tonnes
Deadweight	6611 tonnes
Engine MCR	2380 kW
Propeller type	CPP
Number of propellers	1
Propeller rpm	119

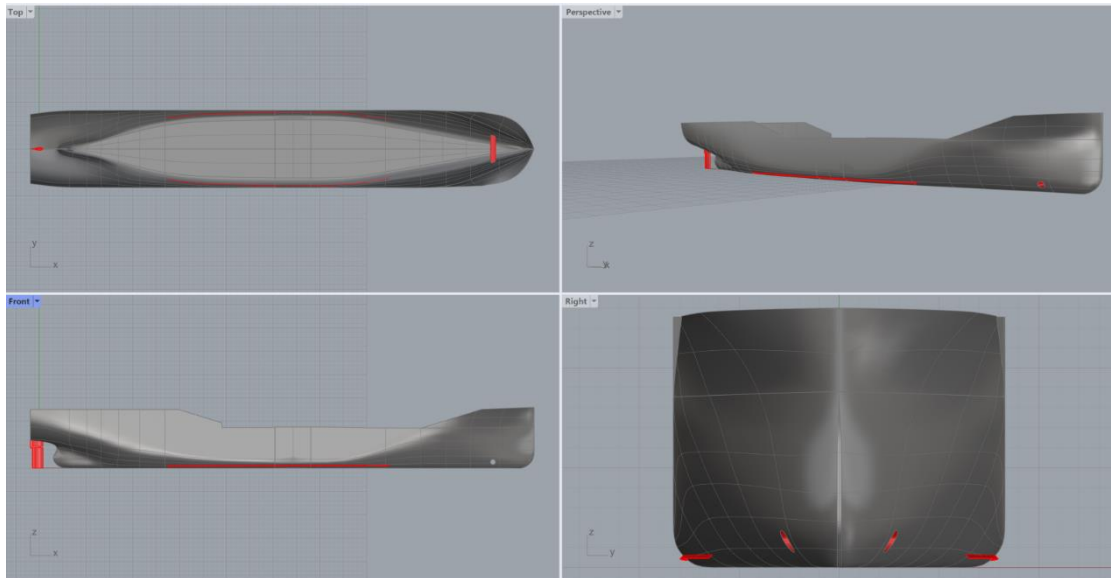


Fig. 2 3-d model of ship hull

3. Sea-trial measurements

Sea-trial measurements on board the pilot ships have been conducted for validating numerical analyses of self-propulsion and manoeuvring under a research campaign aiming to develop a decision support system. In the current context, measurement system and methodology will be presented concerning the monitoring of propulsion parameters.

Delivered shaft power on the ship is obtained by torque and rpm measurements with strain gauge telemetry and laser sensors, respectively. The strain gauge enables the quantification of torque which is then converted to delivered power.

The strain gauges, wireless transponder and batteries and the reflectors for rpm measurement are mounted on the shaft prior to measurements. In Figure 3, installed equipment on the tankers is shown.

On the bridge, an IMU containing dGPS, galvanometer and accelerometers are utilized to acquire the spatial orientation and dynamic attitude of the ship; rudder angle, pitch, wind speed and direction and depth have all been acquired from ship's equipment. Photographs of each have been saved at 1Hz intervals. An in-house OCR software has been used to digitize the data as shown in Figure 5.

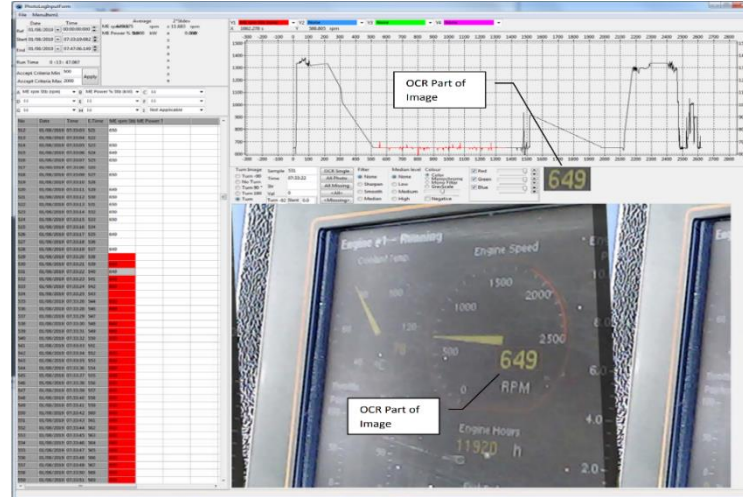


Fig. 5 Screenshot from in-house OCR software

Sea trial for the pilot ship has been conducted on 05/12/2018. The hull of the ship was clean as the final hull cleaning prior to the measurements was reported on 29/09/2018. The ship was loaded to the EEDI draft. True wind speed was in average between 6-8 knots and sea state was reported as 1-2.

4. Numerical methodology

The numerical study on the pilot ship for evaluating the propulsion performance characteristics have been split into three phases. Initially, the resistance of the ship has been predicted in model scale followed by an extrapolation to full-scale. The choice of utilizing the model scale for resistance analyses is associated with the availability of model test results which are used for validation purposes. Separately, open water performance characteristics of the propeller have been investigated. Finally, self-propulsion analyses have been conducted to obtain the self-propulsion point and delivered power. Open water performance predictions and self-propulsion computations are conducted at ship's scale as the results will be compared to shaft power measurements from sea-trials of the ship and its two sisters.

Analyses have been conducted with RANS technique utilizing ANSYS CFX v 19.2 commercial CFD software. The software uses Finite Volume Method to solve the discretized continuity and momentum equations with a vertex centered approach. Advection scheme and turbulence numerics are "high resolution" which forces the solver to adjust the order of the related scheme to the highest possible. The blend factor values are varied across the solution domain depending on the local flow characteristics ensuring boundedness [20]. Throughout all the analyses, turbulence modelling has been achieved by SST model. Previous experience gained by the utilization of this method suggests that the viscous flow around the ship is well represented with this type of turbulence modelling even in the existence of flow separation [21]. Resistance and open water analyses have been conducted with steady state modelling whereas self-propulsion analyses were modelled as unsteady.

4.1 Resistance analyses

Initially, resistance analyses have been conducted for a shorter variant of the current pilot tanker (100 mt in length, 6000 DWT) for which model experiment results were available. The results of these analyses have been compared to experimental data for validation of the numerical model. Following these computations, resistance analyses for the naked hull were conducted for the actual pilot ship with a length of 107.7 mt (6600 DWT). As the process is identical, modelling phases of the actual pilot ship is presented for simplification purposes.

Tanker resistance analyses have been conducted at 1/20 scale. The multi-phase problem has been solved with Volume of Fluid method. The vessel is left free to sink during the computations. Analyses have been conducted at a draft corresponding to 6.5 m at ship's scale for two speeds. This draft is identical to the draft of the model experiments.

The 3-d model of the hull is pre-processed in Rhinoceros and exported to CFD software for solution domain creation. The mesh structure around the bow region of the hull and expected free surface region is shown in Figure 6. The boundary layer modelling along the ship hull is achieved by 12 cells with a growth rate of 1.2. A total of 1,809,429 cells have been used.

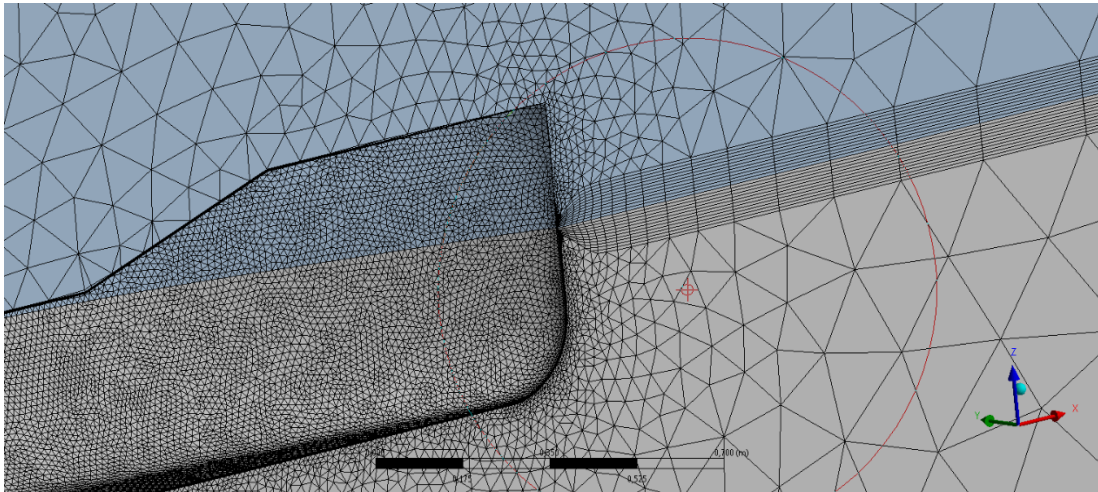


Fig. 6 Mesh structure around the bow and expected free surface

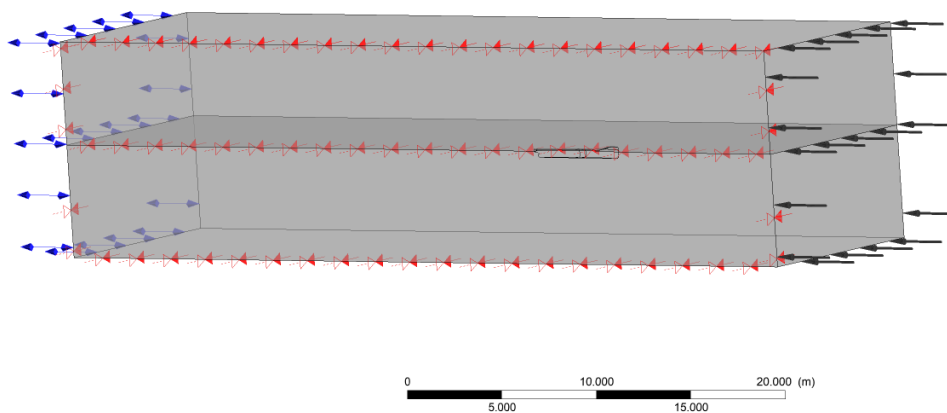


Fig. 7 Solution domain and boundary conditions of resistance analyses

The solution domain and boundary conditions of the resistance analyses are given in Figure 7. The inlet has been positioned 2 ship lengths away from the hull whereas the outlet is

6 ship lengths away. Top and bottom boundaries are 1 ship length deep and side boundary is 2.5 ship length's away from the hull. Due to the symmetric nature of the problem, a half model is utilized with a symmetry boundary condition in the centre plane of the hull. Inlet is modelled as a velocity inlet with fixed inflow speed and 10% turbulence intensity. The top, side and the sea bottom are modelled as free-slip walls and the outlet is specified as opening with hydrostatic pressure definition.

4.2 Open water analyses

Prior to self-propulsion analyses, the performance of the propellers at open water conditions needs to be known. For this purpose, analyses have been conducted at open water conditions to obtain thrust, torque and open water efficiency for the expected range of advance coefficients (J). The obtained data is then used during self-propulsion study.

All open water analyses were conducted at ship scale. The thrust and torque values are obtained from each analysis and are non-dimensionalized to obtain thrust and torque coefficients and open water efficiency.

The propeller model that's been used for the open water and self-propulsion analyses of the pilot tanker is a 4-bladed propeller with a diameter of 4.3 meters. The actual propeller installed on the ship is a 4-bladed CPP type propeller with the same geometrical characteristics.

The solution domain of the open water propeller model accommodates only a single blade due to the periodic nature of the problem. The refinements in the mesh for blades, boss and shaft may be seen in Figure 8. 12 cells have been used for the discretization of the boundary layer along the blade with a growth rate of 1.2 A total of 2,217,102 cells have been used in the model.

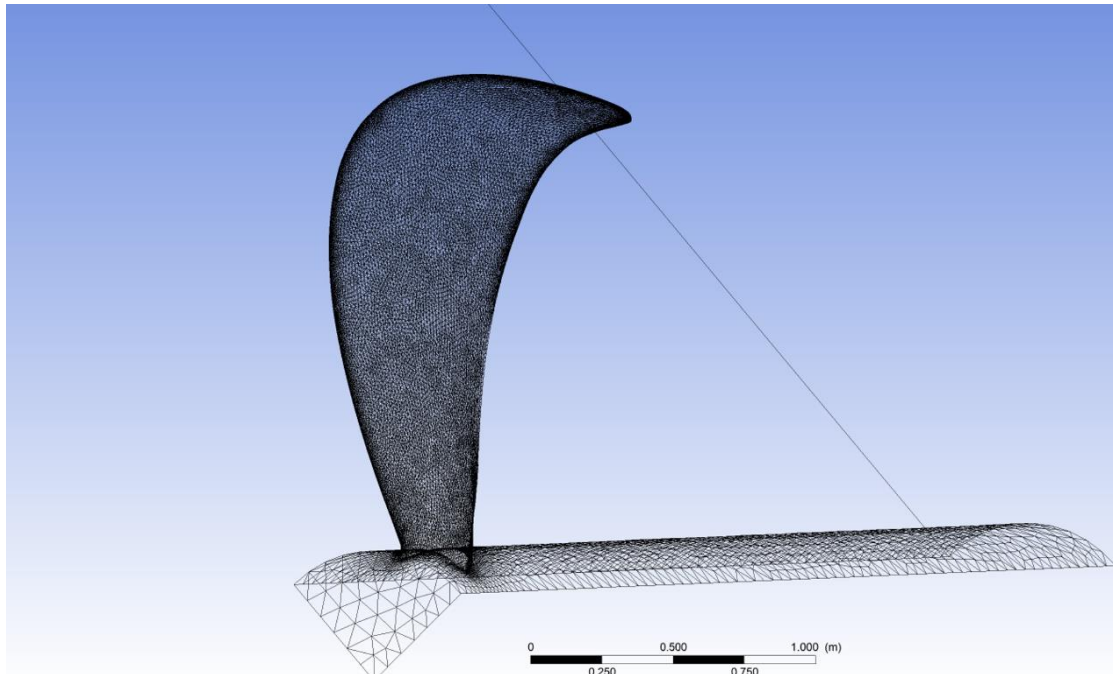


Fig. 8 Mesh structure in way of propeller and shaft

Open water analyses have been conducted for advance coefficients ranging between 0.4 and 0.8. Solution domain and boundary conditions are depicted in Figure 9. The inlet is positioned 5 meters away from the blade which corresponds to the approximate shaft length. Outlet is 3.5 propeller diameters away and the top boundary has a radius of 2 propeller

diameters. The inlet is a velocity inlet with fixed inflow velocity and outlet is modelled as an opening. The top boundary is set as a free-slip wall. The boundaries with the wavy arrows in Figure 9 indicate the rotationally periodic regions. The propeller blade is rotating around the x-axis as shown in the Figure 9. The rotation is modelled via the RFR (rotating frame of reference model) by which problems involving rotation around an axis at a specified angular velocity may be solved. When this model is activated, the solver computes the additional Coriolis and centrifugal components in the momentum equations [20].

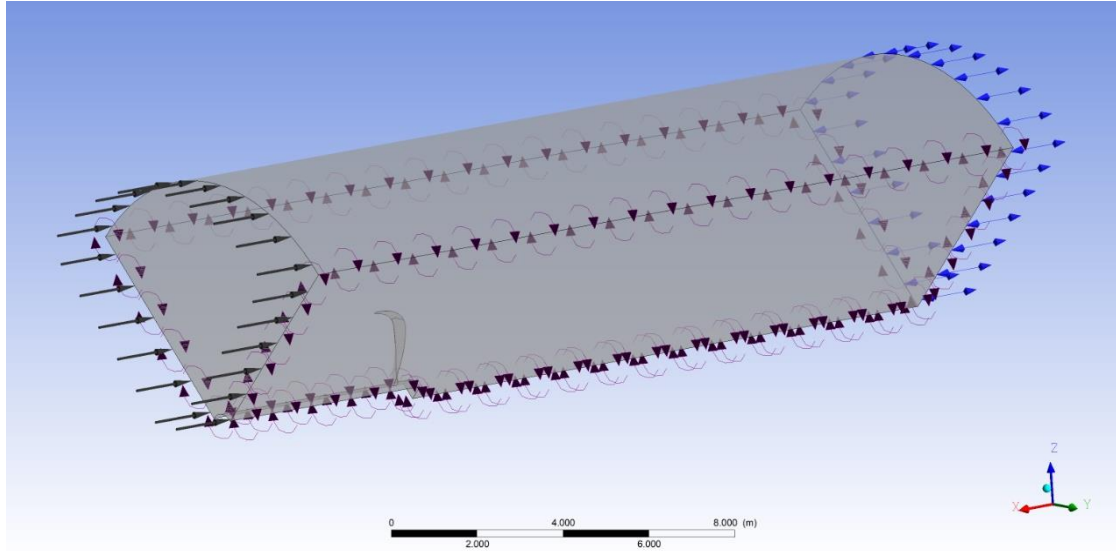


Fig. 9 Solution domain and boundary conditions for open water analyses

4.3 Self-propulsion analyses

The final phase of the numerical analyses is comprised of self-propulsion analyses. For this purpose, a solution domain including the hull and the propellers need to be prepared. These models are prepared in Rhinoceros and exported to CFD software for further processing. The self-propulsion problem is handled as a single-phase problem within this research campaign and hence only the underwater part has been modelled. The mesh details are given in Figure 10. Boundary layer modelling of the hull, propeller and rudder is comprised of 12 cells with a growth rate of 1.2. A total of 15,503,157 cells have been used.

In this study, British method for obtaining the self-propulsion point has been utilized. With this method, the loading of the propeller is varied at the specified ship speed. At least two runs need to be conducted, one where the propeller is under-loaded and one over-loaded [22]. The thrust and variation of the hull resistance hence thrust deduction is monitored and the loading (rpm) at which total resistance and delivered thrust balance is sought.

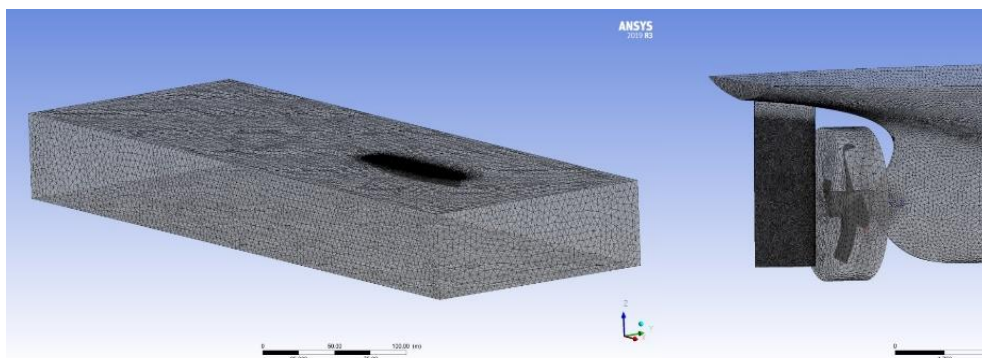


Fig. 10 Mesh details for self-propulsion analyses

The boundary conditions and the solution domain are shown in Figure 11. The inlet is positioned 1 ship length away from the hull whereas the outlet is 3 ship lengths away. Sides and bottom boundaries are placed 0.75 ship length away from the hull. Sides and sea bottom are modelled as free-slip walls whereas the top boundary is modelled as a symmetry plane. Outlet of the domain is modelled as an opening. Inlet is modelled as a velocity inlet with fixed inflow speed.

Interface modelling between the rotating and stationary domains are shown in Figure 12. Self-propulsion analyses of the tanker have been conducted at ship's scale for 12.5 knots. As the analyses are conducted with unsteady (transient) modelling, the meshes in the rotating regions are sliding with the specified angular velocity and the boundaries shown with arrows in Figure 12 serve as interfaces between the rotating and stationary models. Transient rotor-stator interface modelling has been used enabling proper interaction between stationary and rotating domains which is vital for self-propulsion analyses as the interaction between the hull and the propellers need to be captured with high accuracy. By using this type of interface between rotating and stationary domains, fluid particles can proceed to the rotating domain via the interface at their “corresponding position”, ensuring continuous particle tracks. This is achieved by accounting for the comparative orientation of the sliding and stationary domains at the specific time step [20].

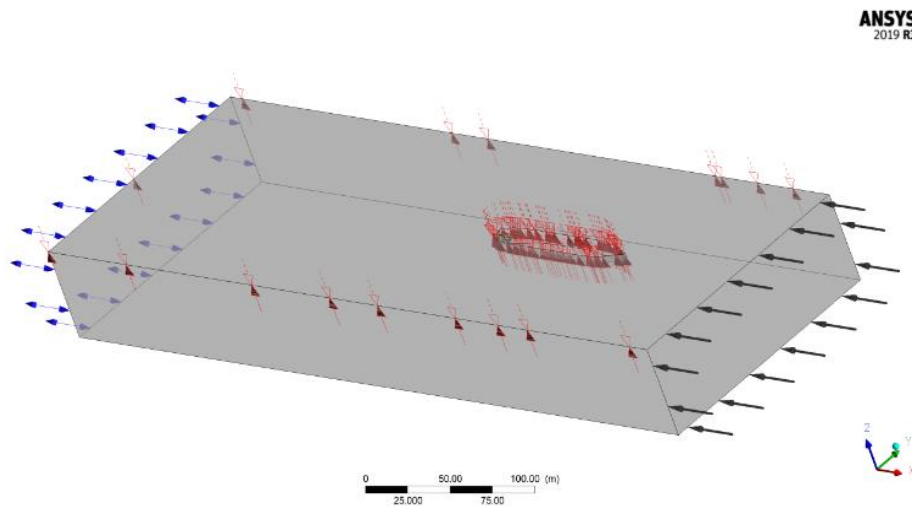


Fig. 11 Solution domain and boundary conditions for self-propulsion analyses

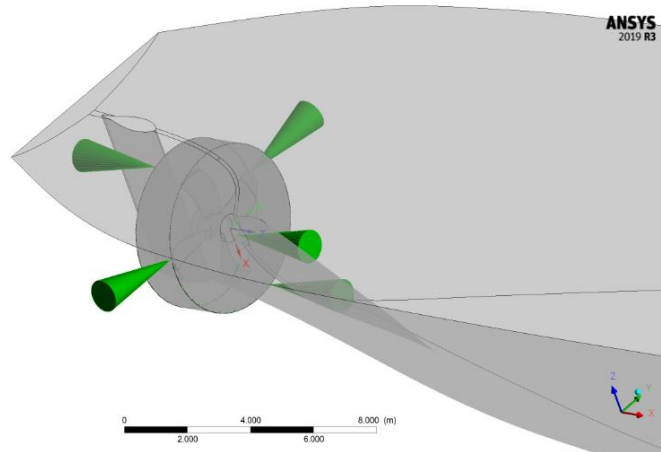


Fig. 12 Interface modeling for self-propulsion analyses

5. Results and discussions

In this section, the results obtained from the numerical analyses for prediction of the resistance, open water propeller performance and self-propulsion performance of the tanker will be presented alongside sensitivity analyses results. Comparisons are also going to be made with sea trial results of the pilot ship and two sister ships.

5.1 Resistance analyses

As previously stated, a shorter variant of the pilot tanker has been tested in a model basin and naked hull resistance computations for the mentioned variant have been conducted accordingly. The experiments have been conducted with a scale of 1/24.5 on a towing tank with dimensions of 160m, 6m, 4.5m.

The resistance analyses for the shorter tanker variant have been conducted for speeds corresponding to 11.5 and 12.5 knots at ship's scale. The resistance data obtained from the analyses of the shorter variant of the pilot tanker at 1/20 scale have been extrapolated to ship's scale and effective power predictions have been obtained as given in Figure 13. ITTC-1978 method has been used for extrapolation of resistance data [23]. In this methodology, the total resistance coefficient of a ship is expressed as:

$$C_{TS} = (1+k)C_{FS} + \Delta C_F + C_A + C_W + C_{AAS} \quad (1)$$

where C_{FS} is the frictional resistance coefficient of the ship, k is the form factor, C_W is the wave resistance coefficient, C_A is the correlation allowance and C_{AAS} is the air resistance coefficient respectively.

In Figure 13, the predicted effective power values are compared with experimental results, and it is seen that a good agreement exists between the experimental and predicted values. The overprediction by CFD is 1.07% and 2.91% for 11.5 and 12.5 knots respectively. As the agreement between the data is suitable for proceeding to pilot tanker analyses, the resistance analyses of the actual pilot tanker have been conducted with analogous approach for speeds corresponding to 11.5 and 12.5 knots at ship's scale.

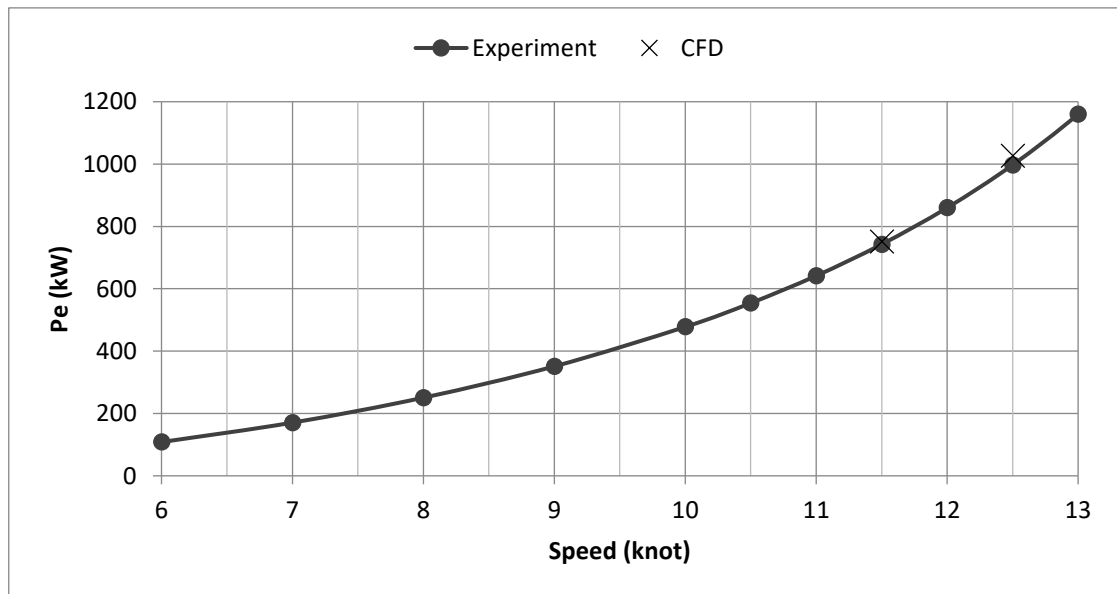


Fig. 13 Effective power comparison for shorter tanker variant

5.2 Open water analyses

Open-water performance predictions have been conducted for advance coefficients ranging from 0.4 to 0.8. Non-dimensional thrust and torque coefficients as well as open water efficiency have been obtained for further use in self propulsion analyses.

Advance coefficient is defined as the ratio of advance velocity over diameter and rps of the propeller such as $J = \frac{V_A}{nD}$ where V_A is the speed of advance, n is the revolution rate of the propeller and D is the diameter of the propeller. The thrust (T) and torque (Q) produced by the propeller is expressed with non-dimensional form as thrust coefficient and torque coefficient. The open-water performance of the propeller is assessed by using thrust coefficient, torque coefficient and the open water efficiency which are denoted as K_T , K_Q , and η_o , respectively:

$$K_T = \frac{T}{\rho n^2 D^4} \quad (2)$$

$$K_Q = \frac{Q}{\rho n^2 D^5} \quad (3)$$

$$\eta_o = \frac{J K_T}{2\pi K_Q} \quad (4)$$

The predicted open water performance data for the propeller of the pilot tanker have been plotted in Figure 14.

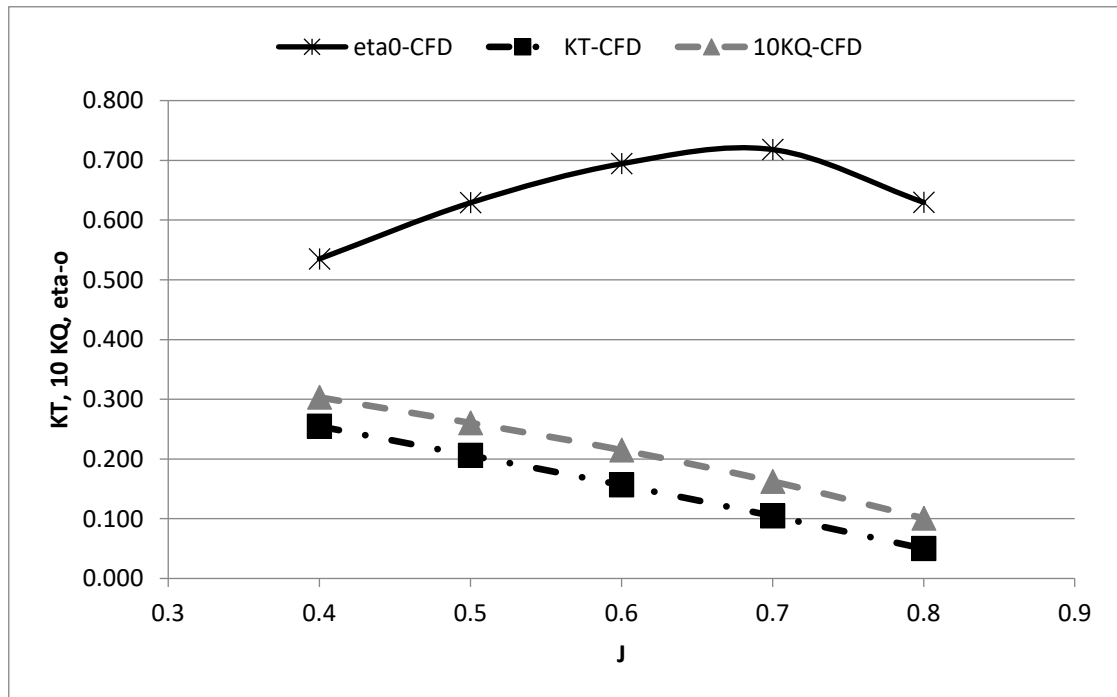


Fig. 14 Open water performance predicted for the stock propeller of tanker

5.3 Uncertainty quantification

A verification study on the grid and time sensitivity of the utilized method needs to be conducted for assessing the fidelity of the proposed methodology of self-propulsion computations. For this purpose, the uncertainty levels on the forces acting on the appended hull

subject to propeller action have been evaluated. The uncertainty analysis has been based on the procedure recommended by ITTC [24]. The details of the procedures have been provided in the study of uncertainty quantification by Ayyıldız and others [1].

Grid sensitivity analyses have been performed on three different grid sizes for a time step of 0.01 s. The grid size has been changed by the refinement ratio r_i which has been determined as $\sqrt{2}$. The time sensitivity has also been studied with three different time steps for the medium grid size. The refinement ratio for time sensitivity has been taken as 0.5. The total number of elements for the grid sensitivity and the time steps for the time sensitivity analyses have been provided in Table 2.

Table 2 Number of total elements and time steps for uncertainty analyses

Number of total elements			Time steps (s)		
$r_I=\sqrt{2}, t=0.01$			$r_I=0.5, \text{medium grid}$		
Fine	Medium	Coarse	Fine	Medium	Coarse
22,564,976	15,530,157	9,859,086	0.0025	0.05	0.01

Both time and grid sensitivity analyses have been performed on the hull with rudder and propeller. The vessel speed has been set to 12.5 knots and the propeller rpm has been set at 118. The resistance of the hull, rudder, and shaft, the thrust and the torque of propeller have been monitored separately. The numerical simulation results for the grid sensitivity (S_{G1} , S_{G2} , and S_{G3}) and time sensitivity (S_{T1} , S_{T2} , and S_{T3}) have been provided in Table 3.

Table 3 Results of sensitivity simulations

	Grid Sensitivity			Time Sensitivity		
	Fine (S_{G1})	Medium (S_{G2})	Coarse (S_{G3})	Fine (S_{T1})	Medium (S_{T2})	Coarse (S_{T3})
Resistance (kN)	-168.52	-167.11	-164.83	-166.59	-166.69	-167.11
Thrust (kN)	210.91	209.66	199.48	209.29	209.34	209.66
Torque (kNm)	117.34	118.74	106.82	118.49	118.60	118.74

The convergence ratios for this study has been evaluated based on the numerical simulations results by using recommended formula as below [24]:

$$R_i = \frac{S_{i2} - S_{i1}}{S_{i3} - S_{i2}} = \frac{\varepsilon_{i,21}}{\varepsilon_{i,32}} \quad (5)$$

The convergence ratio provides the convergence type according to following conditions:

- (i) Monotonic convergence for $0 < R_i < 1$,
- (ii) Oscillatory convergence for $-1 < R_i < 0$,
- (iii) Monotonic divergence for $1 < R_i$,
- (iv) Oscillatory divergence for $R_i < -1$.

For cases with monotonic convergence, the procedure also recommends evaluating the error ($\delta_{i,1}^*$), the order of accuracy (p_i), the correction factor (C_i) by using the generalized Richardson Extrapolation (RE) as follows:

$$\delta_{i,1}^* = C_i \delta_{REi,1}^* \quad (6)$$

$$\delta_{REi,1}^* = \frac{\varepsilon_{i,21}}{r_i^{p_i} - 1} \quad (7)$$

$$p_i = \frac{\ln\left(\frac{\varepsilon_{i,32}}{\varepsilon_{i,21}}\right)}{\ln(r_i)} \quad (8)$$

$$C_i = \frac{r_i^{p_i} - 1}{r_i^{p_{i,est}} - 1} \quad (9)$$

Where $P_{i,est}$ is the estimated order of accuracy which is 2 in this study. The uncertainty (U_i) and the corrected uncertainty (U_{ci}) have been calculated as:

$$U_i = \left(|C_i| + |1 - C_i| \right) \left| \delta_{REi,1}^* \right| \quad (10)$$

$$U_{ci} = |1 - C_i| \left| \delta_{REi,1}^* \right| \quad (11)$$

The verification uncertainty for simulations (U_{SN}) has been evaluated as:

$$U_{SN} = U_G^2 + U_T^2 \quad (12)$$

where U_G and U_T are the grid and time uncertainty, respectively. The uncertainty quantification parameters as Ri , $\delta_{i,1}^*$, $\delta_{REi,1}^*$, p_i , C_i , U_{ci} have been provided in Tables 4, 5 and 6 for resistance and thrust, and torque respectively.

Table 4 Grid and time sensitivity data for the verification of resistance

	Ri	$\delta_{i,1}^*$	$\delta_{REi,1}^*$	p_i	C_i	U_{ci}
Grid Sensitivity	0.621	1.411	2.311	1.375	0.611	0.899
Time sensitivity	0.239	-0.330	-0.031	2.064	1.061	1.069

Table 5 Grid and time sensitivity data for the verification of the thrust

	Ri	$\delta_{i,1}^*$	$\delta_{REi,1}^*$	p_i	C_i	U_{ci}
Grid Sensitivity	0.122	-1.242	-0.173	6.071	7.199	1.070
Time sensitivity	0.132	0.014	-0.007	2.922	2.192	0.008

Table 6 Grid and time sensitivity data for the verification of torque

	Ri	$\delta_{i,1}^*$	$\delta_{REi,1}^*$	p_i	C_i	U_{ci}
Grid Sensitivity	-0.117	N/A	N/A	N/A	N/A	N/A
Time sensitivity	0.786	-36.667	-403.333	0.348	0.091	366.667

Monotonic convergence has been achieved for force parameters (resistance and thrust) with respect to grid and time as obtained R_i values are between 0 and 1. Results have been compared with findings of Degiuli et al [25]. They have assessed the uncertainty of resistance for grid and time step for 3 different motor yacht hull models. The results of both studies indicate that numerical uncertainties are lower than 1.1 %. However, torque convergence with respect to grid was observed to be oscillatory. Therefore, the uncertainty has been based on oscillation maximum (S_U) and minimum (S_L) as shown below:

$$U_i = \frac{1}{2}(S_U - S_L) \quad (13)$$

The corrected simulation results ($S_c = S_{i,l} - \delta_{i,l}^*$) and the uncertainties have been given in the Table 7. For grid sensitivity on torque, corrected results are not provided, and uncertainty has been given as percentage of simulation result.

Table 7 Corrected simulation results and the uncertainties

	Resistance		Thrust		Torque	
	S_c	U_c (% S_c)	S_c	U_c (% S_c)	S_c	$U(S_2\%),$ $U_c(S_c\%)$
Grid Sensitivity	-169.93(kN)	-0.53%	212.15(kN)	0.50%	N/A	5.02%
Time sensitivity	-166.56(kN)	-0.001%	209.28 (kN)	0.004%	118526 (kNm)	0.309%

5.4 Self-propulsion analyses

Prior to the analyses required for obtaining the self-propulsion point, an initial case needs to be run without any propeller rotation. While this serves as a better initial condition to actual analyses as the boundary layer develops along the hull, it enables the quantification of the force component that needs to be accounted for obtaining the self-propulsion point. As the analyses have been conducted with single-phase modelling, the resistance increments due to wave action and wind has been added manually.

Self-propulsion analyses for the pilot tanker have been conducted at 12.5 knots for 3 different propeller loadings. The convergence history of thrust from the analysis with coarse grid size and time-step of 0.01s at 118 rpm has been shown in the Figure 15. All analyses have been performed for a simulation time of 24 seconds to achieve the required convergence in monitored parameters. Forces in the x-direction on the hull, shaft, rudder, and propeller were observed during the simulations. Each force component has different fluctuation tendencies. Additionally, the mentioned force components behave differently in terms of the required time for achieving force convergence. Whilst the forces on the rudder and shaft converge easily around 15 seconds, the forces on the hull start to converge at after 20 seconds as more time is required for the boundary layer to develop and the interaction between the hull and propeller to converge. As the numerical model is sensitive to the rpm of the propeller, any variation introduced during the computation would results in additional computational time as the propeller-hull interaction is resolved slowly. In the current study, this is eliminated by conducting two runs in under-loaded and over-loaded propeller conditions without introducing rpm variation during the computation.

The Y-plus contours along the hull are depicted in Figure 16. The first cells along the majority of the hull have Y-plus values between 300 and 600. Higher values -approximately up to 700- are seen in the bow region where the boundary layer is developing.

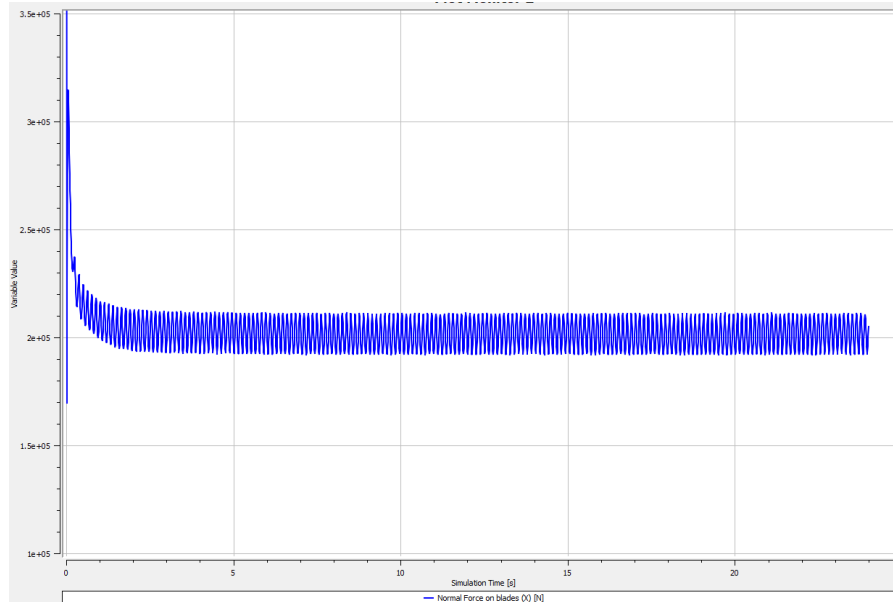


Fig. 15 Convergence history of thrust of the propeller in the analysis of medium grid size and time-step 0.01 for 118 rpm

As previously mentioned, the medium grid has been used with a time-step of 0.01s for the self-propulsion computations. For all runs, the total force in the x-direction has been monitored. By adding the roughness allowance, wave and wind resistance components to the monitored total force, net force in the x-direction is obtained. As the hull has recently been cleaned prior to launching, a new ship hull with a roughness value of 120 microns has been assumed. As depicted in Figure 17, the self-propulsion point is obtained at 118.3 rpm.

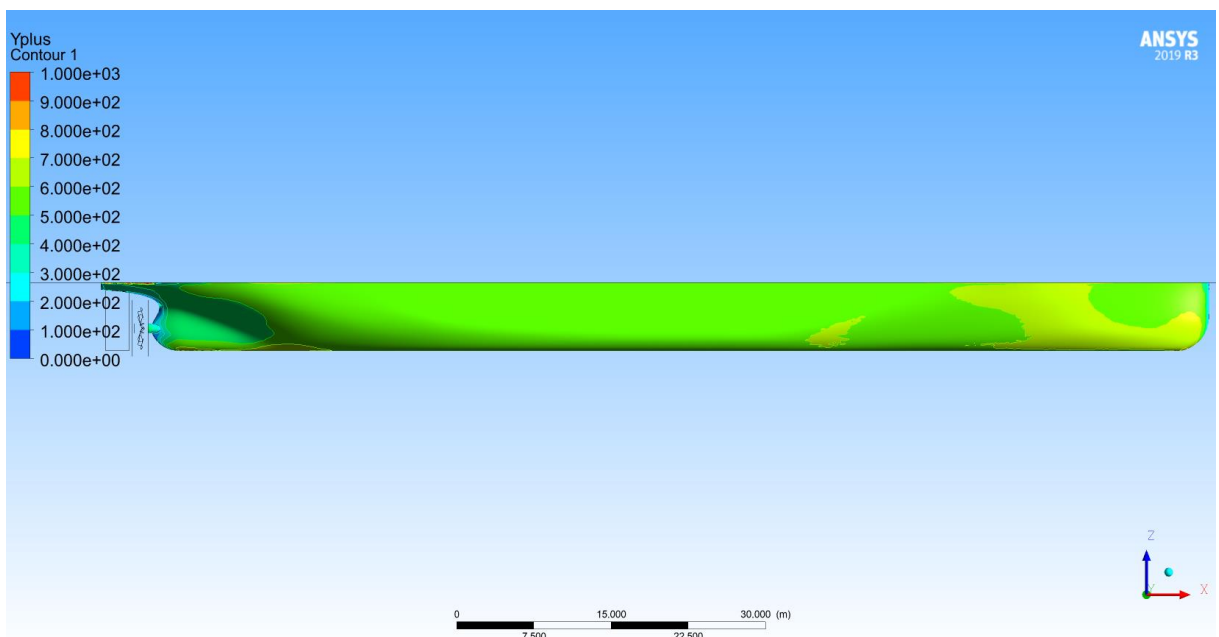


Fig. 16 Variation of Y-plus along the hull

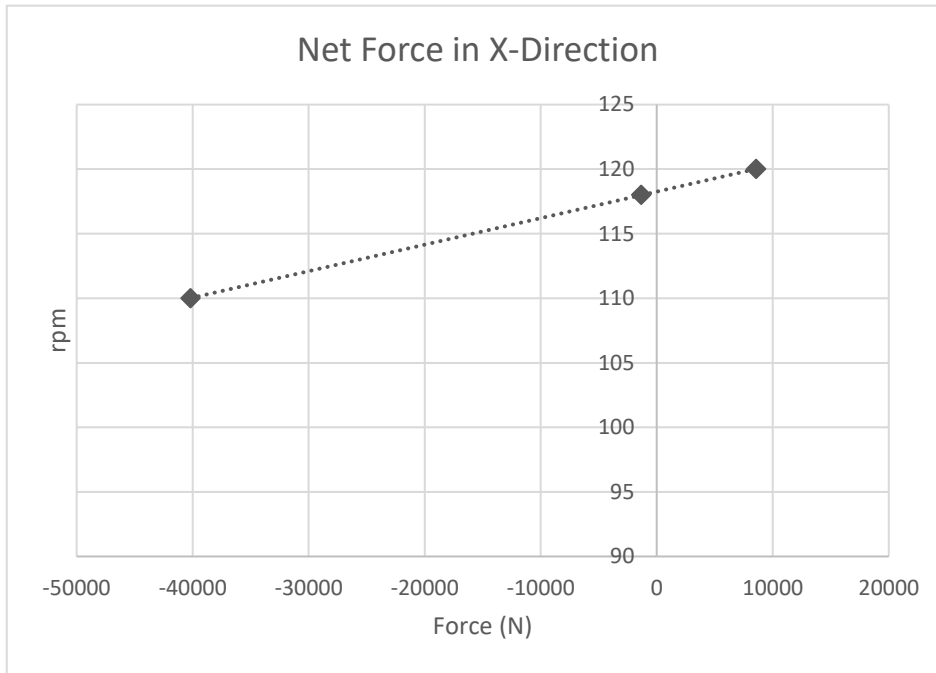


Fig. 17 Variation of net force in x-direction with rpm

The utilized approach incorporates certain engineering assumptions and simplifications as the actual operation on board the ship is different to what has been applied in the numerical approach. Normally, the rpm would be kept constant, and pitch would be varied on board a ship with a CPP type propeller for varying the load on the propeller. In the current numerical approach, a fixed pitch propeller has been utilized and rpm has been varied to change the loading on the propeller. It is assumed that any change in the calculated thrust deduction, wake fraction and relative rotative efficiency values would be negligible depending on the method of varying the loading of the propeller, i.e., changing the pitch or rpm. The change in the calculated performance parameters such as t, w, η_{r-r} is also assumed to be negligible for computation with the numerical and actual propeller as long as the geometric characteristics of the propellers are comparable. This enables the calculations to be conducted with a numerical propeller with similar geometric characteristics when compared to the actual propeller. During post processing, the advance coefficient and open water efficiency of the actual propeller may be calculated for the required thrust and hence thrust coefficient, and power predictions may be obtained for the case with the actual propeller. It is also assumed that the resistance due to wind and wave action may be added manually while obtaining the self-propulsion point with a single-phase simulation, which bears the assumption that the propeller-free surface interaction is negligible.

The increment in the resistance is used to obtain required thrust and actual obtained thrust is equal to the required thrust at the rpm at which the net force in the x-direction is zero. The resistance, thrust and propeller torque for the final self-propulsion point is obtained by interpolation between the results of the closest two runs. As thrust and rpm is known, KT is calculated. Once KT is known, J, Va, w, η_{a-h} and η_{a-0} may easily be obtained. The ratio of the open water torque to propeller torque at self-propulsion point at the same advance coefficient yields η_{r-r} and hence delivered power P_d may be obtained.

The wake profile has also been investigated alongside power prediction. In Figure 18, nominal and effective wake contours are depicted for 12.5 knots of ship speed. With the aid of the post-processing software, the average velocity on the propeller plane at self-propulsion

condition is predicted as 5.22 m/s. During the self-propulsion calculations, advance velocity (V_a) has been calculated as 5.17 m/s from predicted thrust, by obtaining KT and J respectively. The good agreement shows that the data obtained from the proposed calculation method is very close to the actual operating conditions of the propeller predicted by the proposed method.

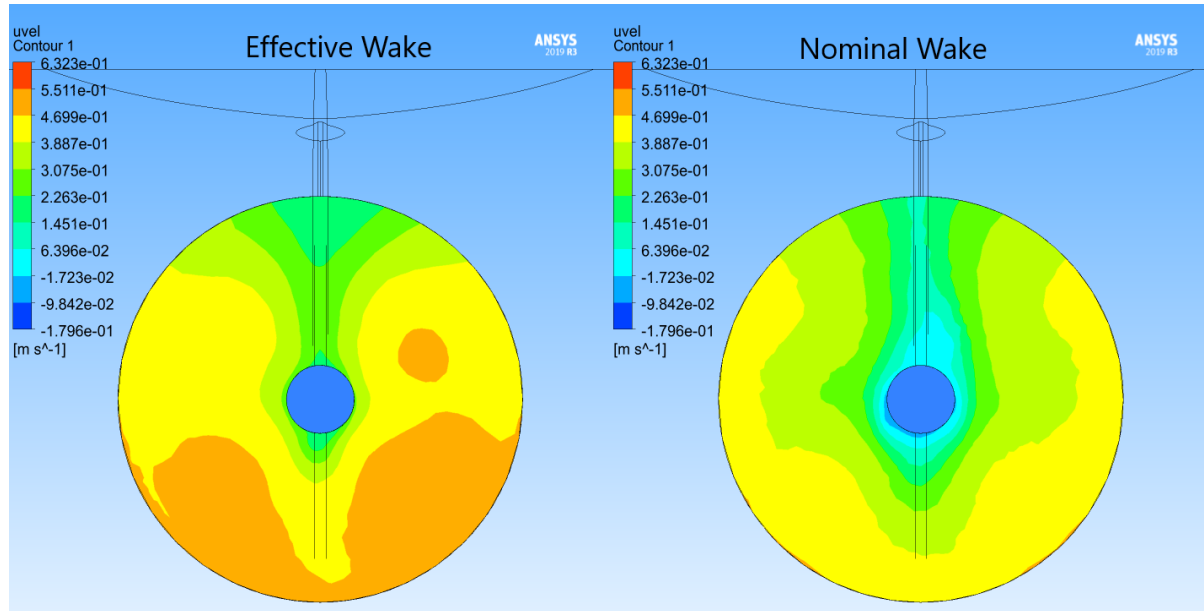


Fig. 18 Nominal and effective wake contours at propeller plane

The results obtained from self-propulsion analyses have been used to predict K_T , J , K_Q , η_{a-0} , η_{a-r} , w , t , η_{a-h} and P_d . The delivered power with the stock propeller is predicted as 1459 kW. Replacing the stock propeller with the actual CPP propeller, the predicted delivered power becomes 1595 kW. Also considering the transmission losses, the brake power required to propel the ship at 12.5 knots is predicted as 1512 kW with the stock propeller. When the stock propeller is replaced with the actual propeller, the required brake power becomes 1653 kW. Results are given in Table 8.

Table 8 Self-propulsion parameters with the numerical and actual propeller

	<i>rpm</i>	<i>KT</i>	<i>J</i>	<i>eta-h</i>	<i>eta-0</i>	<i>eta-r</i>	<i>Pd kW</i>	<i>Pb kW</i>
Numerical propeller	118.3	0.155	0.610	0.986	0.704	1.065	1459	1512
Actual propeller	118.3	0.155	0.558	0.986	0.644	1.065	1595	1653

5.5 Comparison with sea-trial data

The delivered power requirement predicted from self-propulsion computations have been compared to sea-trial data obtained for the pilot ship and two more sisters ships, as given in Figure 19. It is seen that the delivered power values of two sisters are very close to each other across the speed range. As the sea trials of the third ship have been conducted in relatively adverse weather conditions, even the results that have been corrected for adverse weather condition effects are not in agreement with the results of the other two sister ships. The difference between the delivered power values is at the order of 5%. To properly evaluate the differences in these results, uncertainties associated with measurements in actual sea conditions need to be taken into account. Zaho & Wang and Zhou [26] have made towing tests of a large

model in real sea and obtained an uncertainty of 4% for the total resistance. Jang et al [27] have assessed the performance of the propeller in pitch motion with CFD and found that the thrust and torque coefficients tend to fluctuate substantially after 10 degrees of tilt angle. Additionally, slight variations were observed as the immersed depth of the propeller reduces below half of the propeller diameter. Insel [28] states that uncertainties associated with Beaufort scale is the most significant contributor to the overall uncertainty associated with shaft power in sea trials. He has further quantified that the total uncertainty may reach up to 7-8% at the design speed. The differences observed in the sea trial results of the current campaign are in agreement with Insel's findings obtained from sea trials of a set of 12 sister ships.

Considering the above, two approaches may be utilized for comparison of computational data and sea trial results. The delivered power data from all sister ships may be averaged or the data from the two ships with close results may be utilized for comparison, extracting the results of the ship that was tested in adverse weather conditions. The second option has been chosen within this study. As seen in Figure in 19, the delivered power value obtained from the computation is in very good agreement with the sea trial results.

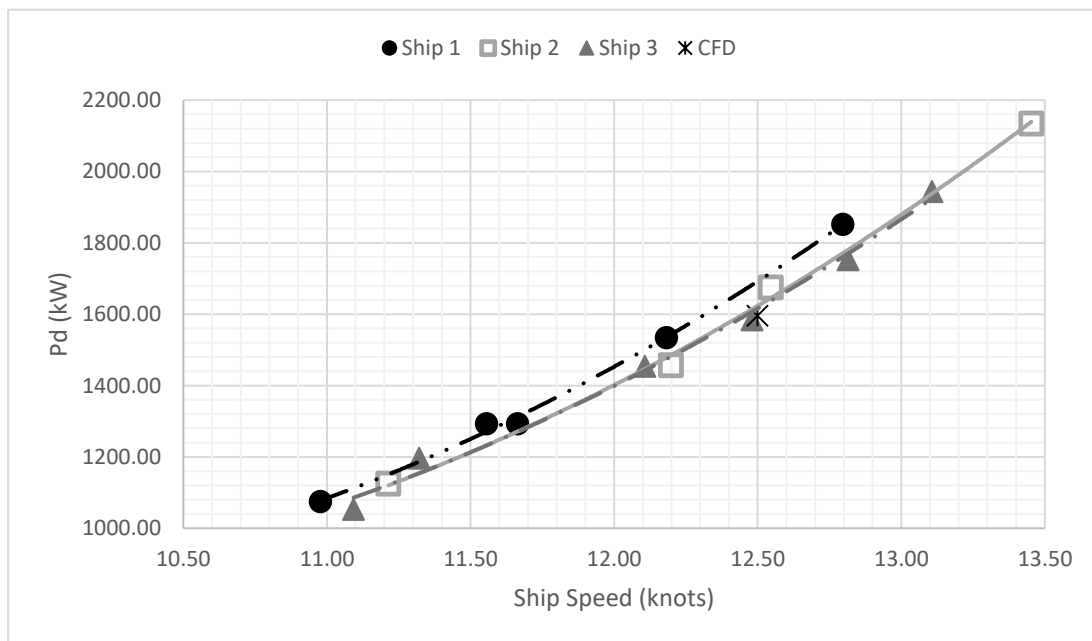


Fig. 19 Delivered powered versus speed – CFD prediction and sea trial data for 3 sister ships

6. Conclusion

Resistance, open water propeller performance and self-propulsion analyses have been conducted with RANS-CFD for a single-screw tanker. Resistance analyses have been compared with experimental data and delivered power predictions have been compared with delivered power measurements at sea-trials. For the tanker ship, data from sea-trials of 3 sister ships have been used. Uncertainty on the force components and propeller torque have been quantified.

Resistance of the naked ship hull has been predicted with model scale analyses and extrapolated to ship's scale. Comparisons of predicted effective power with experimental data indicated a good agreement with a maximum error of 4.13%. It is seen that the errors tend to increase with increasing speed. Although a direct uncertainty assessment has not been made within the scope of this study, previous attempts on quantifying uncertainty for resistance computations and experiments indicate that solutions may be validated.

A direct comparison of open water performance predictions has not been made within the scope of this study as the stock propellers utilized for computations differ from the actual units. The thrust deduction effect is largely correlated with hull design and positioning of the propellers on the hull. It has been assumed that the differences of the pressure variation induced on the hull by stock and actual propellers would be negligible as long as geometric properties are close to each other. Further investigations on the validity of this assumption requires self-propulsion calculations with actual propellers.

The power predicted for the tanker has been compared to sea-trials results of 3 sister ships. The power predicted with proposed method agrees well with the sea trial data. The good agreement between the numerical results and full-scale power measurements should be treated cautiously as both include sources of uncertainties. An error of 4% is present in resistance predictions. The numerical uncertainty on forces (resistance and thrust) is at the order of 0.5%. The major contributor to the numerical uncertainty is the propeller torque which shows an oscillatory convergence characteristic. The uncertainty associated with propeller torque is calculated as 5%. The delivered power value is directly influenced by the predicted torque as it affects the relative rotative efficiency. Therefore, it may be assumed that the calculated uncertainty is directly affecting the predicted delivered power. As previous studies suggest that uncertainties on sea trials measurements may reach 8%, it can be said that the proposed methodology is capable of predicting delivered power with acceptable accuracy.

Results obtained with the proposed methodology of conduction at least two self-propulsion runs, with an under-loaded and over-loaded propeller at ship's scale may also be used for predicting the propulsion performance of the ship under different environmental conditions such as at high wind speeds where more thrust would be required to maintain a certain speed. This method also enables the prediction of propulsion performance of the hull and propeller at reduced loading of the propeller. Such a case is experienced when the ship is propelled with both the propeller and a wind-assist device. As the ship speed will be constant and the propeller will run at a reduced loading in this condition, the propulsion performance of the ship at numerous equilibrium conditions may be predicted easily with the proposed method by a limited number of computations.

Further evaluation of the proposed methodology may be made by scrutinizing the process in more detail. This requires the assessment of the results at each consecutive stage, i.e., evaluating the resistance, thrust and torque at ship scale. This may be realized by measurement of thrust on-board the ship.

ACKNOWLEDGMENTS

This research campaign has been conducted under the financial support of The Scientific and Technological Research Council Of Turkey (TUBITAK) as part of the project entitled "Development of an Artificial Neural Network Based Decision Support System for Ship Energy Efficiency". The financial support of the Council is greatly appreciated.

The authors would also like to acknowledge the support of Acechem Tankers for allocating their vessels for measurements.

REFERENCES

- [1] Ayyıldız, M., Saydam, A. Z., Özbulut, M., 2019., A Numerical Study on the Hydrodynamic Performance of an Immersed Foil: Uncertainty Quantification of RANS and SPH Methods. *Computers & Fluids*, 191. <https://doi.org/10.1016/j.compfluid.2019.104248>
- [2] Ponkratov, D., Zegos, C., 2015. Validation of Ship Scale CFD Self-Propulsion Simulation by the Direct Comparison with Sea Trials Results. *Fourth International Symposium on Marine Propulsors SMP'15*, 289-299. Texas, USA.

- [3] Kinaci, O.K., Gokce, M.K., Alkan, A.D. Kukner, A., 2018. On self-propulsion assessment of marine vehicles. *Brodogradnja*, 69(4), 29-51. <https://doi.org/10.21278/brod69403>
- [4] Mikkelsen, H., L. Steffensen, M., Ciortan, C., Walther, J. H., 2019. Ship scale validation of CFD model of self-propelled ship. *MARINE 2019 Computational Methods in Marine Engineering VIII*, 718-729. Göteborg: International Center for Numerical Methods in Engineering.
- [5] Vukcevic, V., Jasak, H., Gatin, I., Uroic, T., 2017. Ship Scale Self Propulsion CFD Simulation Results Compared to Sea Trial Measurements. *VII International Conference on Computational Methods in Marine Engineering MARINE 2017*. Nantes, France.
- [6] Jasak, H., Vukcevic, V., Gatin, I., Lalovic, I., 2019. CFD validation and grid sensitivity studies of full scale ship self propulsion. *International Journal of Naval Architecture and Ocean Engineering*, 11(1), 33-43. <https://doi.org/10.1016/j.ijnaoe.2017.12.004>
- [7] Sun, W., Hu, Q., Hu, S., Su, J., Xu, J., Wei, J., Huang, G., 2020. Numerical Analysis of Full-Scale Ship Self-Propulsion Performance with Direct Comparison to Statistical Sea Trail Results. *J. Mar. Sci. Eng.* 8, 24. <https://doi.org/10.3390/jmse8010024>
- [8] Mikkelsen, H., Walther, J. H., 2020. Effect of roughness in full-scale validation of a CFD model of self-propelled ships. *Applied Ocean Research*, 99, 102162. <https://doi.org/10.1016/j.apor.2020.102162>
- [9] Li, P., Han, Y., Dong, Z., Zhao, L., 2016. Hydrodynamic Performance Prediction and Sea Trial Verification for the Modification of Propeller Trailing Edge. *The 26th International Ocean and Polar Engineers*. Rhodes: International Society of Offshore and Polar Engineers.
- [10] Hasselaar, T. W., Xing-Kaeding, Y., 2017. Evaluation of an energy saving device via validation speed/power trials and full scale CFD investigation. *International Shipbuilding Progress*, 63, 169-195. IOS Press. <https://doi.org/10.3233/ISP-170127>
- [11] Kamal, I. M., Shamsuddin, M. S., Binns, J., 2018. A Simplified Computational Fluid Dynamics Approach for a Self-propelled Ship Using the Actuator Disc Theory. *Engineering Applications for New Materials and Technologies. Advanced Structured Materials*, 85, 523-539. Springer. https://doi.org/10.1007/978-3-319-72697-7_43
- [12] Dogrul, A., 2022. Numerical prediction of scale effects on the propulsion performance of Joubert BB2 submarine. *Brodogradnja*, 73(2), 17-42. <https://doi.org/10.21278/brod73202>
- [13] Dai, K., Li, Y., Gong, J., Fu, Z., Li, A., Zhang, D., 2022. Numerical study on propulsive factors in regular head and oblique waves. *Brodogradnja*, 73 (1), 37-56. <https://doi.org/10.21278/brod73103>
- [14] Wang, J. H., Zhao, W. W., Wan, D. C., 2016. Self-propulsion Simulation of ONR Tumblehome Using Dynamic Overset Grid Method. <https://www.sci-en-tech.com/ICCM2016/PDFs/1499-5539-1-PB.pdf> Accessed 29th July 2022.
- [15] Song, S., Demirel, Y. K., Atlar, M., 2020. Penalty of Hull and Propeller Fouling on Ship Self-propulsion Performance. *Applied Ocean Research*, 94, 102006. <https://doi.org/10.1016/j.apor.2019.102006>
- [16] Farkas, A., Degiuli, N., Martić, I., 2018. Assessment of Hydrodynamic Characteristics of a Full-Scale Ship at Different Draughts. *Ocean Engineering*, 156, 135-152. <https://doi.org/10.1016/j.oceaneng.2018.03.002>
- [17] Farkas, A., Degiuli, N., Martić, I., Dejhalla, R., 2019. Numerical and Experimental Assessment of Nominal Wake for a Bulk Carrier. *Journal of Marine Science and Technology*, 24, 1092-1104. <https://doi.org/10.1007/s00773-018-0609-4>
- [18] Pena, B., Huang, L., 2021. A Review on the Turbulence Modelling Strategy for Ship Hydrodynamic Simulations. *Ocean Engineering*, 241, 110082. <https://doi.org/10.1016/j.oceaneng.2021.110082>
- [19] Terziev, M., Tezdogan, T., Incecik, A., 2022. Scale Effects and Full-Scale Ship Hydrodynamics: A Review. *Ocean Engineering*, 245, 110496. <https://doi.org/10.1016/j.oceaneng.2021.110496>
- [20] ANSYS, 2013. *Ansys CFX Solver Modelling Guide*. Canonsburg: ANSYS, Inc.
- [21] Saydam, A. Z., Gökçay, S., İnsel, M., 2018. CFD based vortex generator design and full-scale testing for wake non-uniformity reduction. *Oean Engineering*, 153, 282-296. <https://doi.org/10.1016/j.oceaneng.2018.01.097>
- [22] Machado, T. A., 2018. Self-propulsion CFD calculations using the Continental Method, *MSc Thesis*, University of Rostock.
- [23] ITTC, 2017. 1978 ITTC Performance Prediction Method, 7.5-02-03-01.4. <https://www.ittc.info/media/8017/75-02-03-014.pdf> accessed 04 October 2022.
- [24] ITTC, 2017. Uncertainty Analysis in CFD Verification and Validation Methodology and Procedures, 7.5-0.3-01-01. <https://www.ittc.info/media/8153/75-03-01-01.pdf> accessed 29th July 2022.

- [25] Degiuli, N., Farkas, A., Martić, I., Zeman, I., Ruggiero, V., Vasiljević, V., 2021. Numerical and experimental assessment of the total resistance of a yacht. *Brodogradnja*, 72(3), 61-80. <https://doi.org/10.21278/brod72305>
- [26] Zhao, D.G., Wang, Y.W., Zhou, G.L., 2020. Uncertainty analysis of ship model resistance test in actual seas. *Brodogradnja*, 71 (4), 81-94. <https://doi.org/10.21278/brod71406>
- [27] Jang, Y., Eom, M., Paik, K., Kim, S., Song, G., 2020. A numerical study on the open water performance of a propeller with sinusoidal pitch motion. *Brodogradnja*, 71(1), 71-83. <https://doi.org/10.21278/brod71105>
- [28] İnsel, M., 2008. Uncertainty in the analysis of speed and powering trials. *Ocean Engineering*, 35, 1183-1193. <https://doi.org/10.1016/j.oceaneng.2008.04.009>

Submitted: 24.07.2022. Ahmet Ziya Saydam, zsaydam@pirireis.edu.tr
Hidroteknik Nautical Design Technologies Ltd., Turkey
Piri Reis University, Turkey
Gözde Nur Küçüküsu
Accepted: 08.11.2022. Mustafa İnsel
Serhan Gökçay
Hidroteknik Nautical Design Technologies Ltd., Turkey